Prospects for Measuring ΔG from Jets at HERA with Polarized Protons and Electrons

A. De Roeck[a], J. Feltesse[b], F. Kunne[b], M. Maul[c], E. Mirkes[d], G. Rädel[e], A. Schäfer[c], and C. Y. Wu[c]

[a] Deutsches Elektronen-Synchrotron DESY, Notkestrasse 85, D-22603 Hamburg, Germany
[b] DAPNIA, CE Saclay, F-91191 Gif/Yvette, France
[c] Inst. f. Theor. Phys., Johann Wolfgang Goethe-Universität, D-60054 Frankfurt am Main, Germany
[d] Inst. f. Theor. Teilchenphysik, Universität Karlsruhe, D-76128 Karlsruhe, Germany
[e] CERN, Div. PPE, CH-1211 Genève 23, Switzerland

Abstract: The measurement of the polarized gluon distribution function $\Delta G(x)$ from photon-gluon fusion processes in electron-proton deep inelastic scattering producing two jets has been investigated. The study is based on the MEPJET and PEPSI simulation programs. The size of the expected spin asymmetry and corresponding statistical uncertainties for a possible measurement with polarized beams of electrons and protons at HERA have been estimated. The results show that the asymmetry can reach a few percent, and is not washed out by hadronization and higher order processes.

1 Introduction

After confirmation of the surprising EMC result, that quarks carry only a small fraction of the nucleon spin, this subject is being actively studied by several fixed target experiments at CERN, DESY and SLAC [1]. So far only the polarized structure functions $g_1(x, Q^2)$ and $g_2(x, Q^2)$ have been measured. These structure functions measure predominately the polarized quark distribution functions, which, as usual, contain a scheme dependent gluon admixture. A specific property of polarized structure functions is that this admixture can be rather large, due to a rather large polarized gluon distribution function $\Delta G(x_g)$, as suggested by the fact that $\alpha_S(Q^2) \int dx_g \Delta G(x_g, Q^2)$ is renormalization group invariant.

The direct measurement of the polarized gluon distribution $\Delta G(x_g, Q^2)$ has become the key experiment in order to understand the QCD properties of the spin of the nucleon. For a collider with polarized electrons and protons with beam energies such as for HERA the measurement of dijet events offers such a possibility[2].

The gluon distribution enters at leading order (LO) in the two-jets production cross section[1] in deep inelastic scattering (DIS) (see Fig. 1), and the unpolarized gluon distribution $G(x_g, Q^2)$

[1]In the following the jet due to the beam remnant is not included in the number of jets.

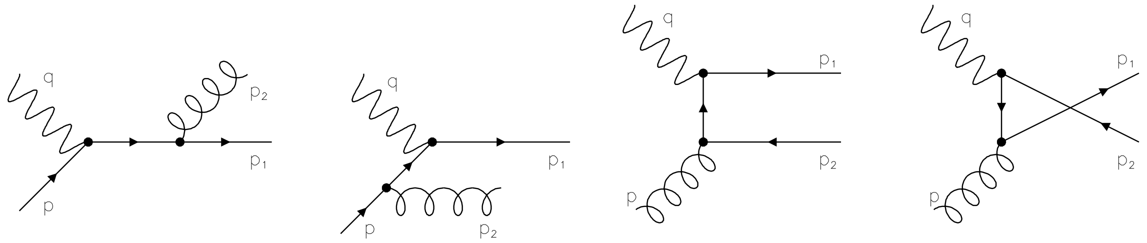

Figure 1: Feynman diagrams for the dijet cross section at LO.

has indeed already been extracted from two-jets events by the H1 collaboration at HERA. With a modest integrated luminosity of 0.24 pb^{-1} collected in 1993, first data on $x_g G(x_g)$ were extracted from dijets events [3] at LO, in a wide x_g range $0.002 < x_g < 0.2$, at a mean Q^2 of 30 GeV^2. These results were found to be in good agreement with the gluon distribution extracted at LO from scaling violations of the structure function F_2. Presently this method is being extended to NLO, and first preliminary results were shown in [4, 5]. An initial study of the feasibility of this measurement for ΔG at HERA (mainly for a polarized fixed target experiment) was presented in [6].

2 Jet cross sections in DIS

Deep inelastic electron-proton scattering with several partons in the final state,

$$e^-(l) + p(P) \rightarrow e^-(l') + \mathrm{remnant}(p_r) + \mathrm{parton}\ 1(p_1) + \ldots + \mathrm{parton}\ n(p_n) \tag{1}$$

proceeds via the exchange of an intermediate vector boson $V = \gamma^*, Z$. Z-exchange and γ^*/Z interference become only important at large Q^2 ($> 1000\ \mathrm{GeV}^2$) and are neglected in the following. We denote the momentum of the virtual photon, γ^*, by $q = l - l'$, (minus) its absolute square by Q^2, and use the standard scaling variables Bjorken-x $x_{Bj} = Q^2/(2P\cdot q)$ and inelasticity $y = P\cdot q/P\cdot l$. The general structure of the *unpolarized* n-jet cross section in DIS is given by

$$d\sigma^{had}[n\text{-jet}] = \sum_a \int dx_a\ f_a(x_a, \mu_F^2)\ \ d\hat{\sigma}^a(p = x_a P, \alpha_s(\mu_R^2), \mu_R^2, \mu_F^2) \tag{2}$$

where the sum runs over incident partons $a = q, \bar{q}, g$ which carry a fraction x_a of the proton momentum. $\hat{\sigma}^a$ denotes the partonic cross section from which collinear initial state singularities have been factorized out (in next-to-leading order (NLO)) at a scale μ_F and implicitly included in the scale dependent parton densities $f_a(x_a, \mu_F^2)$. For *longitudinally polarized* lepton-hadron scattering, the hadronic (n-jet) cross section is obtained from Eq. (2) by replacing $(\sigma^{had}, f_a\ , \hat{\sigma}^a) \rightarrow (\Delta\sigma^{had}, \Delta f_a, \Delta\hat{\sigma}^a)$. The polarized hadronic cross section is defined by $\Delta\sigma^{had} \equiv \sigma^{had}_{\uparrow\downarrow} - \sigma^{had}_{\uparrow\uparrow}$, where the left arrow in the subscript denotes the polarization of the incoming lepton with respect to the direction of its momentum. The right arrow stands for the polarization of the proton parallel or anti-parallel to the polarization of the incoming lepton. The polarized parton distributions are defined by $\Delta f_a(x_a, \mu_F^2) \equiv f_{a\uparrow}(x_a, \mu_F^2) - f_{a\downarrow}(x_a, \mu_F^2)$. Here, $f_{a\uparrow}(f_{a\downarrow})$ denotes the probability to find a parton a in the longitudinally polarized proton whose spin is aligned (anti-aligned) to the proton's spin. $\Delta\hat{\sigma}^a$ is the corresponding polarized partonic cross section.

In the Born approximation, the subprocesses $\gamma^* + q \to q + g$, $\gamma^* + \bar{q} \to \bar{q} + g$, $\gamma^* + g \to q + \bar{q}$ contribute to the two-jet cross section (Fig. 1). The boson-gluon fusion subprocess $\gamma^* + g \to q + \bar{q}$ dominates the two-jet cross section at low x_{Bj} for unpolarized protons (see below) and allows for a direct measurement of the gluon density in the proton. The full NLO corrections for two-jet production in unpolarized lepton-hadron scattering are now available [7] and implemented in the $ep \to n-$jets event generator MEPJET, which allows to analyze arbitrary jet definition schemes and general cuts in terms of parton 4-momenta.

First discussions about jet production in polarized lepton-hadron scattering can be found in Ref. [8], where the jets were defined in a modified "JADE" scheme. However, it was found [7, 9] that the theoretical uncertainties of the two-jet cross section for the "JADE" scheme can be very large due to higher order effects. These uncertainties are small for the cone scheme and the following results are therefore based on the cone algorithm, which is defined in the laboratory frame. In this algorithm the distance $\Delta R = \sqrt{(\Delta\eta)^2 + (\Delta\phi)^2}$ between two partons decides whether they should be recombined into a single jet. Here the variables are the pseudo-rapidity η and the azimuthal angle ϕ. We recombine partons with $\Delta R < 1$. Furthermore, a cut on the jet transverse momenta of $p_T > 5$ GeV in the laboratory frame and in the Breit frame is imposed. We employ the one loop (two loop) formula for the strong coupling constant in a LO (NLO) analyses with a value for $\Lambda_{\overline{MS}}^{(4)}$ consistent with the value from the parton distribution functions. In addition a minimal set of general kinematical cuts is imposed on the virtual photon and on the final state electron and jets. If not stated otherwise, we require 5 GeV$^2 < Q^2 < 2500$ GeV^2, $0.3 < y < 1$, an energy cut of $E(e') > 5$ GeV on the scattered electron, and a cut on the pseudo-rapidity $\eta = -\ln\tan(\theta/2)$ of the scattered lepton (jets) of $|\eta| < 3.5$ ($|\eta| < 2.8$). These cuts are compatible with the existing detectors H1 and ZEUS, and slightly extend the cuts of the H1 gluon analysis from jets.

Let us briefly discuss the choice of the renormalization and factorization scales μ_R and μ_F in Eq. (2). Both the renormalization and the factorization scales are tied to the sum of parton k_T's in the Breit frame,

$$\mu_R = \mu_F = \frac{1}{2}\sum_i k_T^B(i)\ . \tag{3}$$

Here $(k_T^B(i))^2 = 2E_i^2(1-\cos\theta_{ip})$, and θ_{ip} is the angle between the parton and proton direction in the Breit frame. $\sum_i k_T^B(i)$ interpolates between Q, the photon virtuality, in the naive parton model limit and the sum of jet transverse momenta when Q becomes negligible, and thus it constitutes a natural scale for jet production in DIS [9].

Let us first discuss some results for unpolarized dijet cross sections. If not stated otherwise, the lepton and hadron beam energies are 27.5 and 820 GeV, respectively. With the previous parameters and GRV parton densities [10] one obtains a LO (NLO) two-jet cross section σ^{had}(2-jet) of 1515 pb (1470 pb). Thus the higher order corrections are small. This is essentially due to the relatively large cuts on the transverse momenta of the jets. As mentioned before, the boson-gluon fusion subprocess dominates the cross section and contributes 80% to the LO cross section.

In order to investigate the feasibility of the parton density determination, Fig. 2a shows the Bjorken x_{Bj} distribution of the unpolarized two-jet exclusive cross section. The gluon initiated subprocess clearly dominates the Compton process for small x_{Bj} in the LO predictions. The effective K-factor is close to unity for the total exclusive dijet cross section which is the result of compensating effects in the low x ($K > 1$) and high x ($K <1$) regime.

For the isolation of parton distributions we are interested in the fractional momentum x_a of the incoming parton a ($a = q, g$, denoted p in Fig. 1). For events with dijet production x_{Bj} and x_a differ substantially. For two-jet exclusive events the two are related by $x_a = x_{Bj}\left(1 + \frac{s_{ij}}{Q^2}\right)$. where s_{ij} is the invariant mass squared of the produced dijet system. The s_{ij} distribution for the kinematical region under study is shown in Fig. 2b. It is found to exhibit rather large NLO corrections as well. The invariant mass squared of the two jets is larger at NLO than at LO (the mean value of s_{ij} rises to 620 GeV^2 at NLO from 500 GeV^2 at LO).

The NLO corrections to the x_{Bj} and s_{ij} distributions have a compensating effect on the x_a distribution shown in Fig. 2c: the NLO and LO predictions have a similar shape. At LO a direct determination of the gluon density is possible from this distribution, after subtraction of the calculated Compton subprocess. This simple picture is modified in NLO, however, and the effects of Altarelli-Parisi splitting and low p_T partons need to be taken into account more carefully to determine the structure functions at a well defined factorization scale μ_F in NLO.

In the following we discuss some results for polarized dijet production. Our standard set of polarized parton distributions is "gluon, set A" of Gehrmann and Stirling [11], for which $\int_0^1 \Delta G(x)dx = 1.8$ at $Q^2 = 4$ GeV^2. Using the same kinematical cuts as before, the LO polarized dijet cross sections $\Delta\sigma$(2-jet) are shown in the first column of table 1. The negative value for the polarized dijet cross section (–45 pb) is entirely due to the cross section of the boson-gluon fusion process (–53 pb), which is negative for $x_{Bj} \lesssim 0.025$ whereas the contribution from the quark initiated subprocess is positive over the whole kinematical range. Note, however, that the shape of the x_g distribution in the polarized gluon density is hardly (or even not at all) constrained by currently available DIS data, in particular for small x_g. Alternative parametrizations of the polarized gluon distributions in the small x_g region, which are still consistent with all present data [12], can lead to very different polarized cross-sections. The polarized two-jet cross sections for such parton distributions [2] with $\int_0^1 \Delta G(x)dx = 2.7$ and $\int_0^1 \Delta G(x)dx = 0.3$ and at $Q^2 = 4$ GeV^2 are shown in column 2 and 3 in table 1, respectively.

Table 1: LO polarized dijet cross sections for different polarized parton distributions (column 1-3). The contributions from the gluon and quark initiated subprocesses are shown in the last two lines. See text for the details on the kinematics.

	$\int_0^1 \Delta G(x)dx = 1.8$	$\int_0^1 \Delta G(x)dx = 2.7$	$\int_0^1 \Delta G(x)dx = 0.3$
$\Delta\sigma$2-jet	-45 pb	-67.5 pb	-3 pb
$\Delta\sigma^g$2-jet	-53 pb	-76 pb	-10 pb
$\Delta\sigma^q$2-jet	8 pb	8.5 pb	7 pb

The fractional momentum distributions x_a of the incident parton ($a = q, g$), shown in Figs. 2d-f for the three sets of polarized parton densities, demonstrate the sensitivity of the dijet events to the choice of these parametrizations, particularly in the lower x_a range. Note, that the fractional momentum distributions are again related to x_{Bj} by $x_a = x_{Bj}\left(1 + \frac{s_{ij}}{Q^2}\right)$. The corresponding x_{Bj} and s_{ij} distributions are not shown here.

[2]We thank T. Gehrmann for providing us with these parametrizations

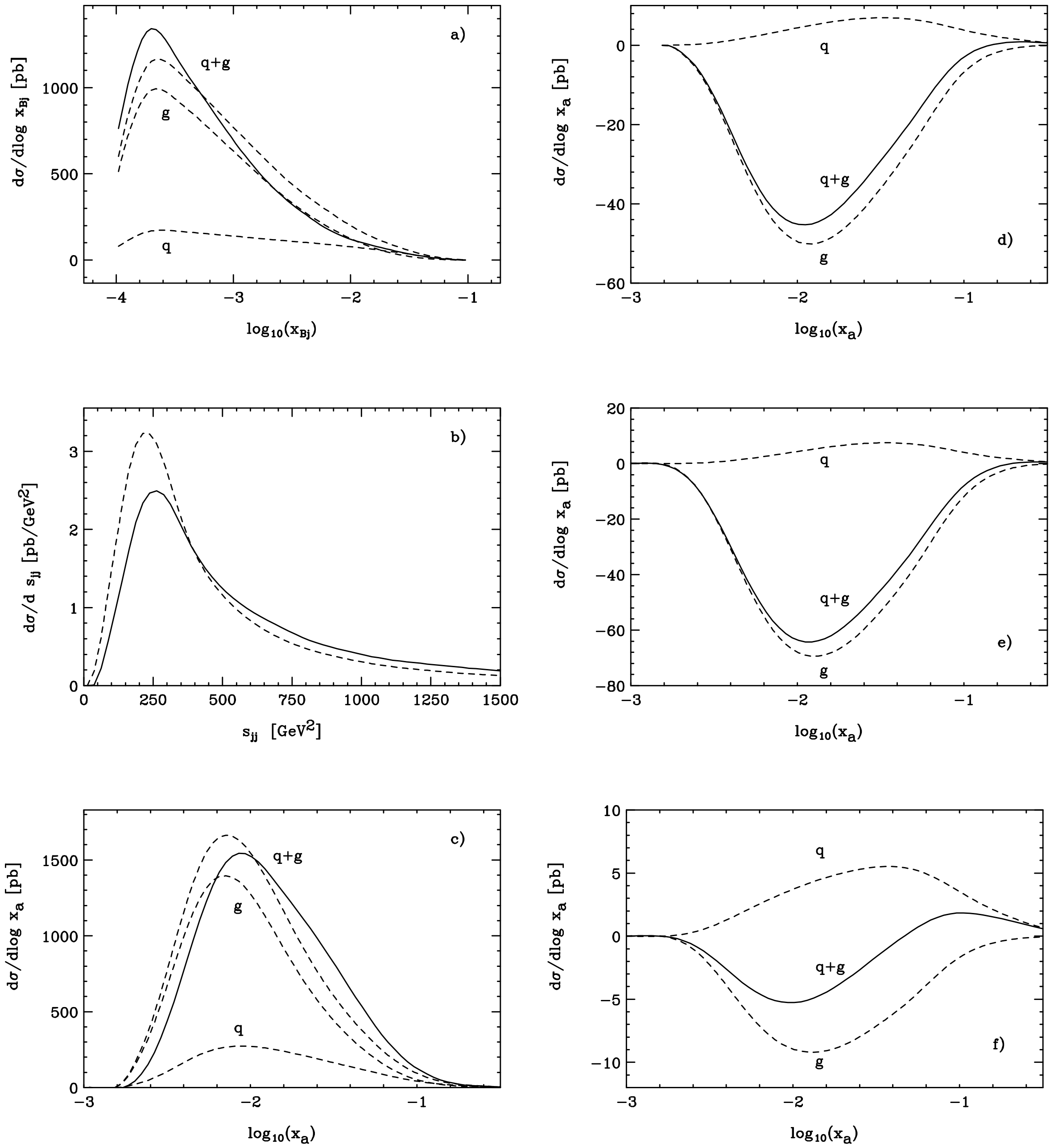

Figure 2: a) Dependence of the *unpolarized* two-jet cross section on Bjorken x_{Bj} for the quark and gluon initiated subprocesses and for the sum. Both LO (dashed) and NLO (solid) results are shown; b) Dijet invariant mass distribution in LO (dashed) and in NLO (solid) for unpolarized dijet production; c) Same as a) for the x_a distribution, x_a representing the momentum fraction of the incident parton at LO; d) Dependence of the LO *polarized* two-jet cross section on x_a for the quark and gluon initiated subprocesses (dashed) and for the sum (solid). Results are shown for the polarized parton distributions "gluon, set A" of Gehrmann and Stirling [11], for which $\int_0^1 \Delta G(x)dx = 1.8$ at $Q^2 = 4$ GeV^2; e) same as d) for $\int_0^1 \Delta G(x)dx = 2.7$ at $Q^2 = 4$ GeV^2; f) same as d) for $\int_0^1 \Delta G(x)dx = 0.3$ at $Q^2 = 4$ GeV^2.

3 Experimental asymmetries

3.1 Parton level studies

In order to study the feasibility and the sensitivity of the measurement of the spin asymmetry at HERA, we have assumed polarizations of 70% for both the electron and the proton beams and statistical errors were calculated for a total luminosity of 200 pb^{-1} (100 pb^{-1} for each polarization).

The expected experimental asymmetry $< A >= \frac{\Delta\sigma^{had}(\text{2-jet})}{\sigma^{had}(\text{2-jet})}$ under these conditions is shown in Fig. 3a, as a function of x_{Bj} and in Fig. 3b-d as a function of x_g. Figures a) and b) correspond to the nominal kinematical cuts defined previously, except for the Q^2 range which was extended to lower values $2 < Q^2 < 2500$ GeV^2 and $10^{-5} < x_{Bj} < 1$. The cross section integrated over all variables is 2140 pb, where 82% of the contribution comes from gluon–initiated events. The asymmetry averaged over all variables is $< A >= -0.015 \pm 0.0015$. It is negative at low x_{Bj} and becomes positive at $x_{Bj} > 0.01$ as expected from Fig. 2.

In Figs. 3c,d a further cut was made: $Q^2 < 100$ GeV^2. This cut permits to reject the positive contributions to the asymmetry coming from high Q^2 (equivalent to high x_{Bj}) events, where the contribution of quark–initiated events is higher. All the remaining events were separated in two bins in s_{ij} –the invariant mass of the dijet– and two bins in y, as the asymmetry and expected NLO corrections are very sensitive to these two variables. Fig.3c corresponds to low invariant masses ($s_{ij} < 500$ GeV^2), and Fig. 3d to high ones ($s_{ij} > 500$ GeV^2). Open points show low y values ($y < 0.6$), and closed points, high y values ($y > 0.6$). In the best case, the asymmetry reaches values as high as 12% (Fig. 3d).

Reducing the beam energy to 410 GeV, instead of the nominal 820 GeV, does not improve the signal in average, although the mean value of y is higher. The asymmetry signal increases only for a few points around $x_g > 0.1$, since a higher incident energy probes slightly higher values of x_g.

3.2 Hadronization and detector effects

So far we discussed cross sections only on the parton level and to lowest order. While, on the level of matrix elements, one can only calculate leading order and next to leading order corrections, in real experiments one always encounters a coherent superposition of contributions of all orders. It is therefore important to investigate next how the picture changes when one takes the effects of higher orders, the fragmentation of the jets into hadrons and detector smearing into account. These effects have been studied in two ways: i) a different program called PEPSI (see below) was used, which is a full LO lepton-nucleon scattering Monte Carlo program for unpolarized and polarized interactions, including fragmentation; ii) parton showers, to emulate the higher orders, and parton fragmentation have been added to the LO matrix elements of MEPJET. PEPSI was further used to study effects of detector smearing.

The PEPSI program is the polarized extension to the unpolarized lepton-nucleon Monte Carlo program LEPTO 6.2 [13]. It adds to the unpolarized cross section, which is a convolution of the partonic cross section σ_p and the unpolarized structure functions $q(x, Q^2)$, the respective

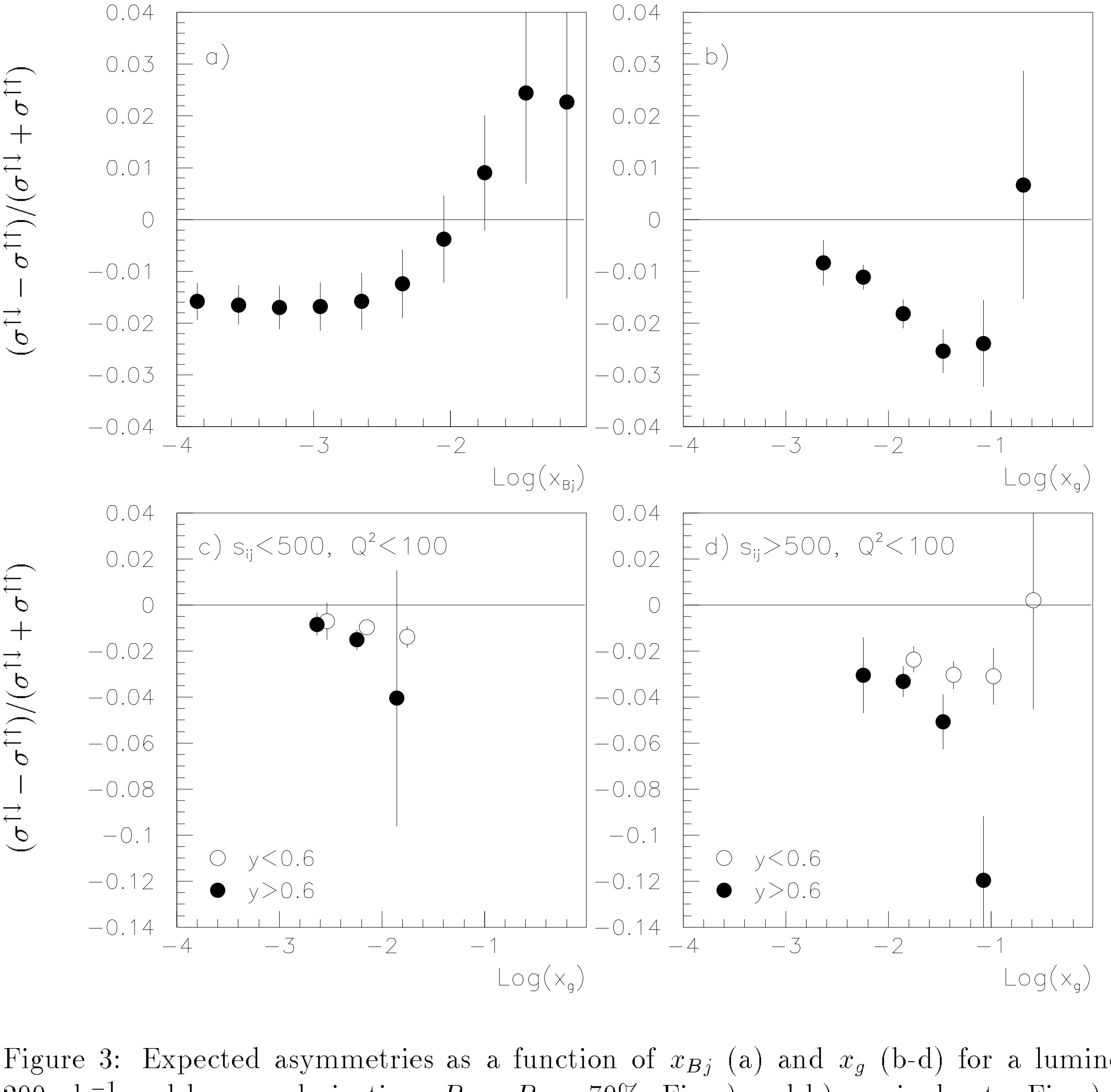

Figure 3: Expected asymmetries as a function of x_{Bj} (a) and x_g (b-d) for a luminosity of 200 pb^{-1} and beam polarizations $P_e = P_p = 70\%$; Fig.a) and b):nominal cuts; Fig.c) and d): $Q^2 < 100$ GeV^2; In Fig.c) and d) data are separated in bins of s_{ij} and y.

polarized cross section as a convolution of the polarized partonic cross section $\Delta\sigma_p$ and the polarized parton densities $x\Delta q(x)$:

$$d\sigma \sim \int_{x_{p,min}}^{x_{p,max}} \frac{dx_p}{x_p} q(x_p/x) d\sigma(x_p, y) + POL \int_{x_{p,min}}^{x_{p,max}} \frac{dx_p}{x_p} \Delta q(x_p/x) d\Delta\sigma(x_p, y) \tag{4}$$

Here x is the Bjorken x_{Bj}, while x_p is defined via $x_p = x_{Bj}/x_a$, with x_a the fraction of the target momentum carried by the initial parton, as defined before. POL is a parameter which is $+1$ for lepton and nucleon spin being antiparallel to each other and -1 in the case where the electron and nucleon spins are parallel to each other. The unpolarized leading order (LO) partonic cross section used already in LEPTO is described in [14], the longitudinally polarized LO cross section is given in [15]. The leading order polarized cross section contains two subprocesses: the gluon bremsstrahlung and the photon-gluon fusion, see Fig. 1. The partons fragment into hadrons via string fragmentation as implemented in JETSET[16]. For the polarized parton density functions there are two different sets [11, 17] implemented which both appertain to the unpolarized parton density functions given in set [10].

Event samples corresponding to 200 pb^{-1} are generated with a similar event selection as for the partonic analysis in Section 3.1. The beam polarizations were taken to be $P_e = P_p = 70\%$. The kinematic region $5 < Q^2 < 2500$ GeV^2, $0.3 < y < 0.8$ was selected (the cut in y corresponds roughly to $E(e') > 5$ GeV). Jets are searched for with the cone algorithm (radius 1) with $p_T > 5$ GeV in the pseudorapidity region $-2.8 < \eta < 2.8$, conform with for example the present H1 detector. The LO 2-jet cross section thus calculated with PEPSI is 1511 pb, 82% of which is contributed by the boson-gluon fusion process. These numbers compare well with those of MEPJET, given in section 2.

To increase statistics we further study jets with $p_T > 4$ GeV, and repeat the studies of section 3.1. This does not change the asymmetries significantly. In Figs. 4a,b the results for the asymmetry are shown as function of x_{Bj} and x_g for similar cuts as in Fig. 3, using the "gluon set A". For Fig. 4b the Q^2 range has been limited to 100 GeV^2. The calculations are shown at the parton level (dashed and dotted lines) and at the detector level (open and closed points). A calorimetric energy resolution of $\sigma_E/E = 0.5/\sqrt{E(\mathrm{GeV})}$ is used to simulate the detector response.

The first observation is that the asymmetries produced by PEPSI are very similar to the ones from MEPJET. Secondly the asymmetry at the detector level is well correlated with the asymmetry at the parton level. This means that present detectors at HERA are well prepared to make this measurement. It was verified that this conclusion still holds with a calorimetric energy resolution which is twice worse. Also a miscalibration of the energy scale of 2%, a number within reach at the time of this measurement, does not disturb the correlation significantly.

The average asymmetry $< A >$ amounts to -0.016 ± 0.002 at the parton level and -0.015 ± 0.002 at the detector level. For the selected kinematic region 40% of the events accepted on the parton level do not enter the detector event sample, and 15% of the final selected events have a parton kinematics outside of the measured region. When the region is restricted to $s_{ij} > 500$ GeV^2 these migrations are reduced to 25% and 12% respectively.

In Fig. 4c,d the results are shown for the asymmetry for a different set of polarized parton distributions: "gluon set C"[11]. These exhibit a smaller asymmetry around $x_g \sim 0.1$ than the "gluon set A", as can be seen from the parton level curves. This difference survives after the detector smearing, and thus measurements of this quantity can help to discriminate between different sets of parton distributions.

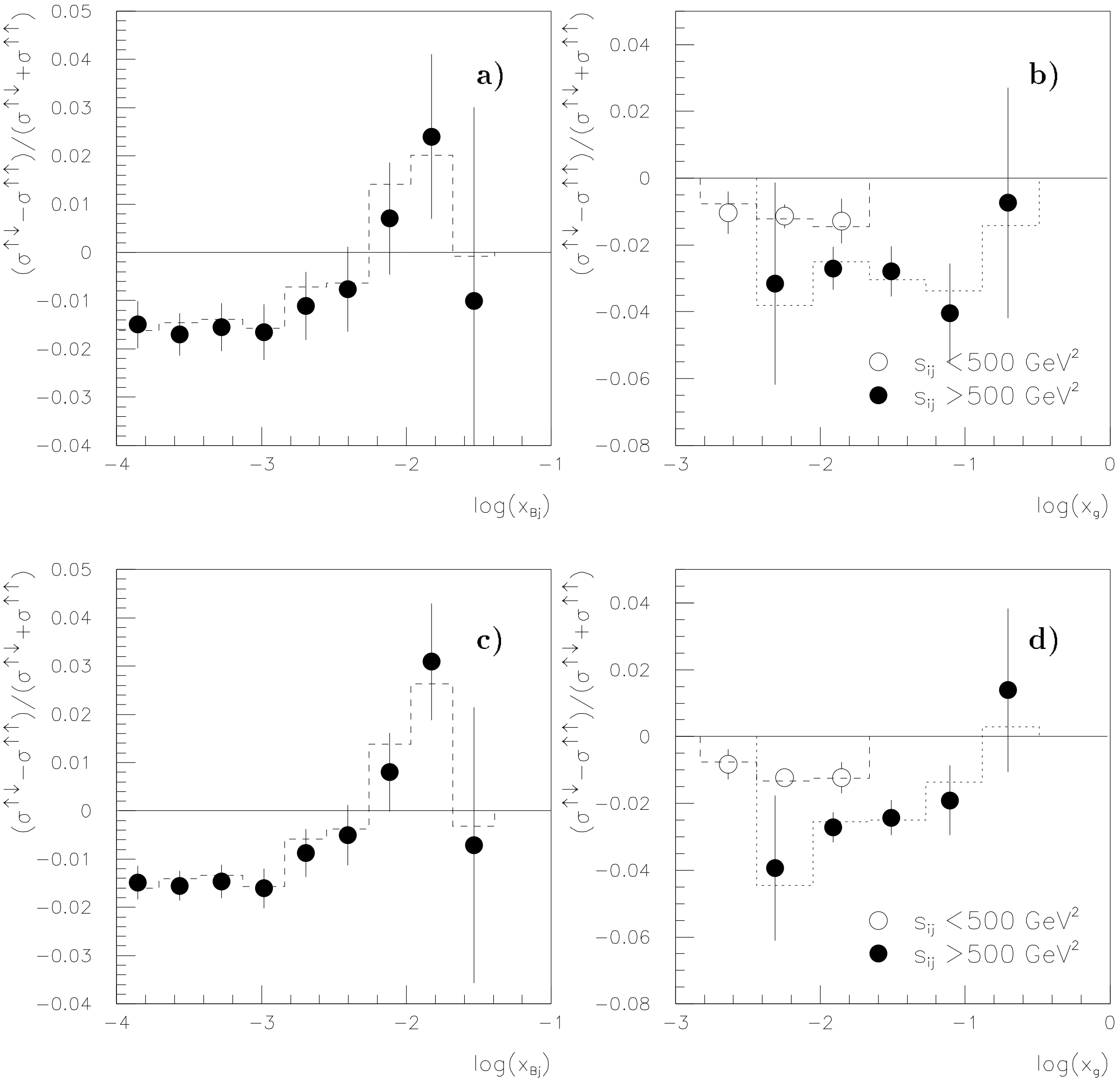

Figure 4: Expected asymmetries as a function of x_{Bj} (a,c) and x_g (b,d) for a luminosity of 200 pb^{-1} and beam polarizations $P_e = P_p = 70\%$. The figures (b,d) have an additional cut $Q^2 < 100$ GeV^2 on top of the nominal cuts, explained in the text. Figs. (a,b) are for the polarized parton set GS-A, Figs. (c,d) for GS-C [11].

3.3 Higher order effects

The studies above were based on a program that includes the LO matrix elements and fragmentation, but no higher order QCD effects. The effect of the latter, and the comparison with the effect of fragmentation, was studied in a dedicated analysis whereby the leading order MEPJET program used in section 2 and 3.1 was supplemented by two packages. The first one is the program PYTHIA57 [18] which simulates higher order effects in the framework or initial and final state parton showering and the second one is the program JETSET74 [16] for hadronization, as used in the PEPSI Monte Carlo.

Following a previous publication[7], the following cuts are used for the kinematic variables: $40 < Q^2 < 2500$ GeV^2, $1 < W^2 < 90000$ GeV^2, $0.001 < x_{Bj} < 1$, and $0.04 < y < 1$. We further impose for the outgoing lepton a cut on the minimal energy of 10 GeV and on the rapidity range $|y| < 3.5$.

Jets are generated via leading order matrix elements with the MEPJET program and then fed into PYHTIA as an external process, which adds initial and final state parton showering. Thus all QCD processes are included except for four-gluon vertices. A more detailed description of parton showering can be found in [19, 20]. For the showering scale, initial and final we used both times Q^2. We will investigate scale dependence in a forthcoming publication. The parton density functions set MRS D–' [21] was taken. For the final hadrons and partons we also choose the rapidity cut $|y| < 3.5$. The jet scheme for detecting hadron and parton jets is the cone scheme as described before with the maximal cone distance one. A sharp cut off of 5 GeV for the jet transverse momentum was taken.

In the showering process jets with small p_T can branch into jets with $p_T > 5$ GeV. The string fragmentation mechanism contributes in a similar way thus enhancing the magnitude of the total cross section within the imposed detector cuts.

Fig. 5 shows the unpolarized inclusive two-jets cross section for the sum of gluon and quark initiated events. The solid histogram shows the differential cross section versus the maximum of p_T for the analyzed two-jet events after parton showering and hadronization. It is in magnitude and shape comparable to the NLO order matrix element calculation by the MEPJET program, represented by the open triangles. A small shift in the direction of small $p_{T,\max}$ is observed, caused by the fragmentation process. The dashed histogram shows the cross section for parton showering without fragmentation. The absolute cross section is smaller than the NLO cross section, but the shapes agree well, without any significant shift. Hence we do not expect that the results calculated with PEPSI, as shown above, will be strongly affected by higher order processes. In comparison, the dotted histogram gives the leading order result from the MEPJET program.

The figure shows that the deviations are significant only for $p_{T,\max}$ smaller than 15 GeV, i.e for soft jets where also next to leading order effects are expected to be large. For larger $p_{T,\max}$ the calculations are in good agreement. The differences between the various curves can serve as a measure for the systematic errors. It has to be noted that the effects of showering and fragmentation are large if and only if the NLO effects are large, too. First studies with higher order effects included in PEPSI confirm that the the asymmetry survives in the presence of parton showers. With the present analysis the asymmetry however reduces to $< A >= 0.009 \pm 0.002$ (parton level) and the shape of the asymmetry distribution as function of x_g changes somewhat with x_g. Improved methods to determine x_g may restore the original distributions and are subject of a future study.

4 Concluding Remarks

The results show that if the assumed luminosity and beam polarizations can be delivered at HERA, the present detectors H1 and ZEUS will be in a comfortable position to measure a spin asymmetry of a few per cent in average, with a few per mile statistical precision, using two-jet events. The asymmetries survive at the hadron and detector level. In order to minimize the experimental systematic uncertainties, it is desirable to have in the HERA ring bunch

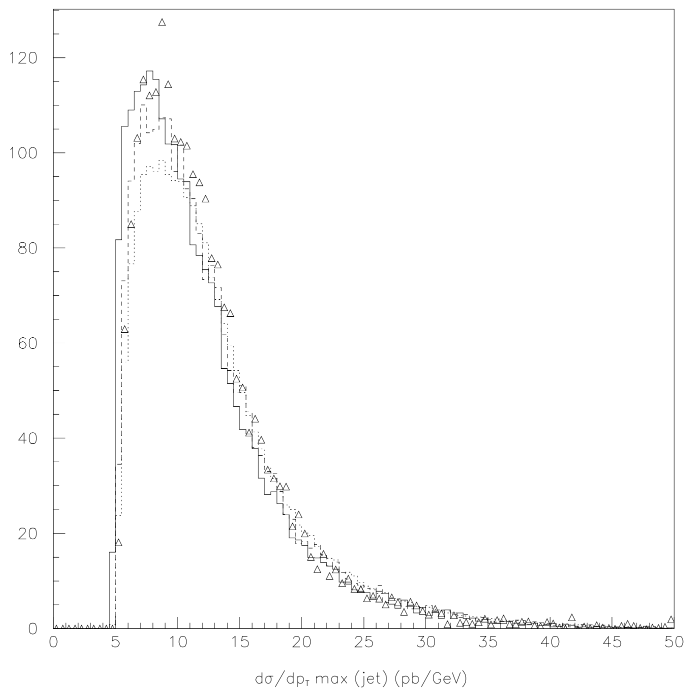

Figure 5: Simulation of higher order and fragmentation effects: triangles: NLO cross section, solid histogram: LO + parton shower + fragmentation, dashed histogram: LO + parton shower, dotted histogram: only LO matrix elements.

trains of protons with alternating helicity. On the theoretical side, NLO QCD corrections are needed. The NLO corrections reduce the renormalization μ_R and factorization scale μ_F dependence (due to the initial state collinear factorization) in the LO calculations and thus reliable predictions in terms of a well defined strong coupling constant and scale dependent parton distributions become possible. At the moment, these corrections are only available for unpolarized jet production [7, 22]. One expects for the asymmetry $< A >= \frac{\Delta\sigma^{had}(2\text{-jet})}{\sigma^{had}(2\text{-jet})}$ that the scale dependence in the individual cross sections partly cancels in the ratio. In fact, varying the renormalization and factorization scales between $\mu_R^2 = \mu_F^2 = 1/16\ (\sum_j k_T^B(j))^2$ and $\mu_R^2 = \mu_F^2 = 4\ (\sum_j k_T^B(j))^2$ in the LO cross sections introduces an uncertainty for the ratio A of less than 2 %, whereas the uncertainty in the individual cross sections is much larger.

In conclusion, the dijets events from polarized electron proton collisions at HERA can provide a good measurement of the gluon polarization distribution for $0.002 < x_g < 0.2$, the region where $x_g \Delta G(x_g)$ is expected to have a maximum.

References

[1] A. Magnon, Contribution to the Workshop DIS96, Rome, 1996.

[2] J.Feltesse, F.Kunne, E.Mirkes, hep-ph/9607336, to appear in Phys. Lett. B.

[3] H1 Collaboration, *Nucl. Phys.* B **449**, 183 (1995).

[4] J. Repond, Contribution to the DIS96 Workshop, Rome (1996).

[5] K. Rosenbauer, Contribution to the DIS96 Workshop, Rome (1996).

[6] W. Vogelsang, in Proceedings of the Workshop 'Physics at HERA', Eds. W. Buchmüller, G. Ingelman, DESY Hamburg (1992), Vol 1, p. 389.

[7] E. Mirkes and D. Zeppenfeld, hep-ph/9511448, Phys. Lett. B **380** (1996) 205; see also these proceedings.

[8] C. Ziegler and E. Mirkes, *Nucl. Phys.* B **429** (1994) 93.

[9] E. Mirkes and D. Zeppenfeld, hep-ph/9606332, in Proceedings of the "QCD and QED in Higher Orders" 1996 Zeuthen Workshop on Elementary Particle Theory, April 22-26, 1996.

[10] M. Glück, E. Reya and A. Vogt, *Z. Phys.* C **67** (1995) 443.

[11] T. Gehrmann and J. Stirling, hep-ph/9512406, *Phys. Rev.* D **53** (1996) 6100.

[12] T. Gehrmann and J. Stirling, private communication.

[13] G. Ingelman, Uppsala internal report TSL/ISV-92-0065 and Proceedings of the Workshop 'Physics at HERA', Eds. W. Buchmüller, G. Ingelman, DESY Hamburg (1992), Vol 3, p. 1366 and references therein.

[14] R. D. Peccei, and R. Rückl, *Nucl. Phys.* B **162** (1980) 125.

[15] L. Mankiewicz, A. Schäfer and M. Veltri, *Comp. Phys. Comm.* **71** (1992) 305.

[16] T. Sjöstrand, *Comp. Phys. Comm.* **39** (1986) 347;
T. Sjöstrand and M. Bengtsson, *Comp. Phys. Comm.* **43** (1987) 367;
see also T. Sjöstrand, CERN-TH 6488/92.

[17] M. Glück, E. Reya, M. Stratmann, W. Vogelsang, *Phys. Rev.* D **53** (1996) 4775.

[18] H. -U. Bengtsson and T. Sjöstrand, *Comp. Phys. Comm.* **46** (1987) 43: see also T. Sjöstrand, CERN-TH 6488/92.

[19] M. Bengtsson, T. Sjöstrand *Z. Phys.* C **37** (1988) 465.

[20] T. Sjöstrand, *Phys. Lett.* B **157** (1985) 321.

[21] A. D. Martin, R. G. Roberts, W. J. Stirling, *Phys. Lett.* B **306** (1993) 145.

[22] E. Mirkes and D. Zeppenfeld, contribution to the Workshop DIS96, Rome, 1996.